

# Entanglement in a continuously measured two-level system coupled to a harmonic oscillator

E. Hernández-Concepción,<sup>1</sup> D. Alonso,<sup>2,3</sup> and S. Brouard<sup>1,3</sup>

<sup>1</sup>Departamento de Física Fundamental II, Universidad de La Laguna, La Laguna E38204, Tenerife, Spain

<sup>2</sup>Departamento de Física Fundamental y Experimental, Electrónica y Sistemas, Universidad de La Laguna, La Laguna E38204, Tenerife, Spain

<sup>3</sup>Instituto Universitario de Estudios Avanzados (IUDEA) en Física Atómica, Molecular y Fotónica,

Facultad de Físicas, Universidad de La Laguna, La Laguna 38203, Tenerife, Spain

(Received 13 October 2008; revised manuscript received 27 January 2009; published 15 May 2009)

The dynamics of a two-level system (TLS) coupled to a harmonic oscillator (HO) is studied under the combined effect of a thermal bath acting on the HO and of a detector continuously measuring one of the components of the spinlike TLS. The analysis focuses on the dynamics of the “relative entropy of entanglement” (REE) in the one-energy-excitation manifold of the reduced TLS+HO system. For this model system, a stationary state is shown to be reached for which the relative entropy of entanglement is in general nonzero, even though, under certain approximations, the separate effects of bath and detector would be to remove any trace of this resource from the system. Analytical as well as numerical results are obtained for the REE as a function of the different parameters involved in the model definition.

DOI: 10.1103/PhysRevA.79.052318

PACS number(s): 03.67.Bg, 42.50.Dv

## I. INTRODUCTION

Entanglement is a quantum resource essential for the field of quantum information processing. Protocols for quantum computation or simulations, quantum teleportation, etc. rely on the ability to generate and control quantum correlations (entanglement) established between different systems or, more generally, different degrees of freedom [1–3]. Many physical systems have been studied in recent years regarding the possibility to implement quantum gates, decoherence-free protocols, entanglement purification protocols, quantum error correction codes, etc., where most of the works analyze possible strategies to isolate and protect the relevant dynamics from the effects of its environment or to compensate for some of them [3–7].

A second step in any protocol designed to manipulate quantum information deals with the interaction of the system with a measuring device, a detector that provides information about the state of the system and exerts some backaction on it. This detector can be considered as another environment from which some information about the system is gained but whose effects on the system has to be controlled or, at least, taken into account [8].

In this paper we focus our study on a prototypical system, namely, a harmonic oscillator (HO) and a two-level system (TLS) coupled by a term proportional to  $x\sigma_x$ , where  $x$  and  $\sigma_x$  represent the position operator for the HO and the  $x$  component of the Pauli vector acting on the Hilbert space of the TLS, respectively. In particular, the amount of entanglement that can be eventually generated on or extracted from a given manifold of the system (TLS+HO) is evaluated when the HO is in contact with a zero-temperature Markovian reservoir and operator  $\sigma_x$  is being continuously measured by an external detector. Different variants of this model have been considered [also under different approximations, such as the rotating wave approximation (RWA) or an adiabatic approximation] to describe physical experiments in the context of optical cavity quantum electrodynamics (QED) [9,10], of

trapped ions [4,11], or in the context of “circuit” quantum electrodynamics (CQED) [12–14] and nanoelectromechanical devices [15–19]. The main results of this work are general enough to be qualitatively applicable to a wide range of systems and interactions.

Coupling a quantum system to a larger, normally uncontrollable, environmental system such as a bath or a detector tends in general to affect it by degrading its coherence and the amount of entanglement it contains. In some cases, however, it is precisely the combined effect of two different baths, the key element, that can be used to generate entanglement as described in [10,20–22]. Our study shows that this is the case when a continuous measurement is performed on part of a system while a zero-temperature Markovian reservoir is coupled to some other part of the same system. The evolution of the reduced system (TLS+HO) is analyzed, assuming that the values of the measured quantity are discarded, so that only the effect that the detector produces onto the combined TLS+HO is relevant. The actual measurement process, which is modeled by means of some interaction of the TLS with a resonator (detector), will be described in some detail in Sec. II.

To characterize quantitatively the quantum correlations established in this system a quantity known as relative entropy of entanglement (REE) [23] is used, whose main features are studied as functions of the different parameters involved. The mechanisms that generate entanglement are normally either oscillatory, meaning that its continuous action creates and destroys entanglement periodically or they loose their efficiency asymptotically under the effect of the different external baths because energy and/or correlations are lost by the system. For the system and environments under study, two competitive mechanisms, of absorption and emission of energy, may drive the system, under certain conditions, to a stationary state for which finite amounts of entanglement in different subspaces of the TLS+HO system are obtained.

This paper is organized as follows. The model system under study is introduced in Sec. II, together with a general

description of its dynamics. In Sec. III, the REE is calculated by means of an analytical expression valid for this model under certain approximations; whereas some numerical results are presented and analyzed in Sec. IV. Finally, in Sec. V, some general conclusions and discussions are presented.

## II. MODEL

Let us consider a two-level system described by the Hamiltonian operator  $H_a = \frac{1}{2}\hbar\omega_a\sigma_z = \frac{1}{2}\hbar\omega_a(|e\rangle\langle e| - |g\rangle\langle g|)$  coupled to a harmonic oscillator,  $H_o = \hbar\omega_o(a^\dagger a + \frac{1}{2})$ , by the interaction term  $H_I = \hbar g\sigma_x(a^\dagger + a) = \hbar g(\sigma_+ + \sigma_-)(a^\dagger + a)$ , where  $\sigma_+ = |e\rangle\langle g|$  and  $\sigma_- = |g\rangle\langle e|$ . Creation and annihilation operators for the HO are denoted by  $a^\dagger$  and  $a$ , respectively, and  $g$  is the coupling strength. The full system Hamiltonian is given by  $H = H_a + H_o + H_I$ . For simplicity, we will focus on the resonant case, where  $\omega_a = \omega_o = \omega$ .

The oscillator is assumed to be interacting with a Markov reservoir in its vacuum state, whereas the two-level system is coupled to a detector that continuously measures  $\sigma_x$ . The case of a thermal bath having a nonzero temperature is briefly discussed in Sec. IV. The master equation that rules the system is then given by [9,24,25]

$$\dot{\rho} = -i[H, \rho]/\hbar - k[\sigma_x, [\sigma_x, \rho]] + \nu\mathcal{D}[a]\rho, \quad (1)$$

where  $\rho$  is the reduced density matrix for the TLS+HO system, and  $\mathcal{D}[a]\rho \equiv 2apa^\dagger - a^\dagger ap - pa^\dagger a$ . The decay rates of the TLS and HO are denoted by  $\nu$  and  $k$ , respectively. Note that the term  $-[\sigma_x, [\sigma_x, \rho]]$  is equivalent to expression  $\mathcal{D}[\sigma_x]\rho$ , according to the fact that the measuring device is being considered as a reservoir that affects the system as information is obtained from it. From now on we set  $\omega=1$ , so that relevant time scales of the system are given by  $g^{-1}$ ,  $k^{-1}$ , and  $\nu^{-1}$ , measured in units of  $\omega^{-1}$ .

The measurement process could be realized for instance in the context of circuit QED by means of a probe resonator that is coupled to the TLS (a Cooper-pair-Box in this case) through an interaction term proportional to  $\sigma_x c^\dagger c$ , where  $c(c^\dagger)$  is the annihilation (creation) operator of the resonator. This interaction is obtained from a Janes-Cummings term  $\hbar\mu(c^\dagger\sigma_- + c\sigma_+)$  [9] by detuning the resonator frequency ( $\omega_r$ ) from that of the TLS by an amount much larger than the coupling constant  $\mu$  (dispersive regime). This procedure leads to an interaction term of the form  $H_d = \hbar(\mu^2/\Delta)\sigma_x c^\dagger c$ , where  $\Delta \equiv \omega_r - \omega_a$ , and the charge basis for the Cooper-pair-Box (TLS) is the eigenbasis of  $\sigma_z$  [13,16,26,27]. The interaction  $H_d$  then induces a frequency shift onto the probe resonator depending on the  $\sigma_x$  eigenstates, which in turn produces a phase shift in the signal carried, e.g., by a transmission line connected to the resonator [16]. This phase shift can be measured continuously with high efficiency [27]. Finally, adiabatic elimination of the resonator, following the standard procedure described in [9,28,29], leads to a term proportional to the double commutator  $[\sigma_x, [\sigma_x, \rho]]$  in the master equation, describing the effect of the measurement on the TLS. The measurement strength obtained after adiabatic elimination of the probe resonator is  $k = \mu^4|\alpha|^2/(\Delta^2\gamma)$ , where  $|\alpha|^2$  is the average number of “phonons” in the detector and  $\gamma$  denotes its decay rate, which, on the other hand, has to be

much larger than the ratio  $\mu^2/\Delta$  for the adiabatic elimination procedure to be valid.

The results presented in this paper are however independent of the detailed form of the interaction between the TLS and the detector. As far as information about  $\langle\sigma_x\rangle$  is obtained from the detector coupled to the TLS, the master equation that describes the evolution of the model system has the form given by expression (1), which is the starting point of our study [30]. For an interaction term of the form  $H_d = \hbar\mu\sigma_x(c^\dagger + c)$ , for instance, the effect of the TLS onto the detector resembles that of an external drive in the  $x$  coordinate of the resonator, depending on the  $\sigma_x$  eigenstates. A measurement of a shift in the position of the resonator will then be equivalent to a measurement of  $\sigma_x$ , leading again to the master Eq. (1).

The Hilbert space is spanned by vectors  $|n, \delta\rangle$ , where  $n$  is an eigenvalue of operator  $a^\dagger a$ ,  $n=0, 1, 2, \dots$ , and  $\delta=e, g$  denote the excited and ground states of the TLS, respectively. For the isolated HO+TLS, under a rotating wave approximation, for which  $H_I^{\text{RWA}} = \hbar g(a\sigma_+ + a^\dagger\sigma_-)$ , operator  $a^\dagger a + \sigma_z/2$  is a constant of motion. The subspace spanned by pairs of its degenerate eigenvectors,  $\{|n, g\rangle, |n-1, e\rangle\}$ , will be denoted as the  $n$ -phonon manifold.

Roughly speaking, the main effect of the measurement process is to drive the system to an incoherent superposition of the two eigenstates of  $\sigma_x$ . The  $\nu$  reservoir pushes the system toward the state  $|n=0\rangle$ , whereas  $H_I$  mixes the populations in each particular phonon manifold and generates coherences. The combination of the different mechanisms and their relative magnitudes are responsible at the end of the appearance of nonzero entanglement in the stationary state and of its actual value.

To the master Eq. (1) different “unravelings” can be associated, each one corresponding to a different stochastic Schrödinger equation (SSE) or stochastic master equation (SME). The effects of the detector on the TLS and of the  $\nu$  reservoir on the HO can be for instance taken into account by means of two complex Gaussian noise variables,  $dW_1$  and  $dW_2$ , such that the ensemble averages satisfy  $dW_1 = dW_2 = 0$ ,  $dW_1^* dW_2 = 0$ , and  $dW_1 dW_1^* = dW_2 dW_2^* = dt$ , with  $dt$  being a small time increment [30,31]. This unraveling leads to the following SSE:

$$\begin{aligned} d|\psi\rangle = & -i(H/\hbar)|\psi\rangle dt - k(\sigma_x - \langle\sigma_x\rangle)^2|\psi\rangle dt + \sqrt{2k}(\sigma_x - \langle\sigma_x\rangle) \\ & \times |\psi\rangle dW_1 + \nu\left(\langle a^\dagger + a\rangle a - a^\dagger a - \frac{1}{4}\langle a^\dagger + a\rangle^2\right)|\psi\rangle dt \\ & + \sqrt{2\nu}\left(a - \frac{1}{2}\langle a + a^\dagger\rangle\right)|\psi\rangle dW_2, \end{aligned} \quad (2)$$

where  $\langle\dots\rangle$  denotes a quantum-mechanical average over the normalized stochastic state  $|\psi\rangle$ . In the context of circuit QED mentioned above, if a homodyne measurement is performed onto the probe resonator field in order to detect its phase shift, then the measurement record is given by  $dr = \langle\sigma_x\rangle dt + (8k)^{-1/2}dW_1$ , as the mean value of  $\sigma_x$  is proportional to the phase shift of the detector. However, no particular measuring scheme needs to be associated in principle to this SSE, since Eq. (2) is used here only as a convenient manner to express

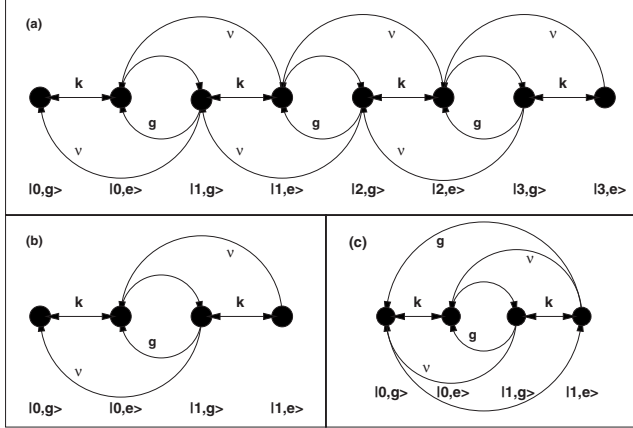


FIG. 1. (a) Graph associated to the dynamics of the system described by Eq. (2) in the case where a rotating wave approximation is assumed for the  $g$  coupling between the TLS and the HO. Relaxation processes and continuous measurement are labeled by  $v$  and  $k$ , respectively. (b) Truncation of the previous graph to the subspace spanned by the set of states  $|0,g\rangle$ ,  $|0,e\rangle$ ,  $|1,g\rangle$ , and  $|1,e\rangle$ . (c) Graph representing the dynamics of the system within the subspace spanned by  $\{|0,g\rangle, |0,e\rangle, |1,g\rangle, |1,e\rangle\}$  when the nonresonant terms are taken into account additionally to those shown in (b).

an evolution equation in the Hilbert space of the system states such that one can get a better intuition on the dynamics that takes place.

Indeed, to Eq. (2) one can associate a graph [see Fig. 1(a)] that helps one to understand the key elements of the dynamics of the system. To each state  $|n, \delta\rangle$  a vertex of the graph is associated. The different vertices are connected by the different terms appearing in Eq. (2), labeled by their corresponding coupling constants. A RWA is used at this point, although the effect of the nonresonant terms will be considered later on.

If the system is initially in the state  $|0,g\rangle$ , for instance, the measurement process will induce the development of a component  $|0,e\rangle$ , which in turn couples through  $H_I$  to state  $|1,g\rangle$ , within the one-phonon manifold. The detector then couples component  $|1,g\rangle$  to the state  $|1,e\rangle$ . The effect of the  $v$  reservoir on the other hand is to relax energy from the system, connecting states  $|1,g\rangle$  and  $|1,e\rangle$  to states  $|0,g\rangle$  and  $|0,e\rangle$ , respectively. Further action of the measuring device drives the system to higher-energy states, connecting the states  $|n,e\rangle$  with the states  $|n,g\rangle$ . Finally, direct interaction between the HO and the TLS mixes the states  $|n-1,e\rangle$  and  $|n,g\rangle$ , within the  $n$ -phonon sector. The cycle is closed by the interaction with the bath, which relaxes energy from the oscillator degree of freedom, driving the state  $|n,\delta\rangle$  to  $|n-1,\delta\rangle$ . Interaction with the detector provides a mechanism for the system to lose energy but also to gain some energy, whereas the coupling  $g$  preserves the energy of the system (if the RWA is assumed). These combined competitive mechanisms lead to a stationary state of the system which will be shown to have in general a finite amount of entanglement (see Fig. 4 below for an example).

In order to gain some insight, a simplified dynamics will be considered, i.e., for  $g \ll \omega, k, v$ . In that case it is sufficient

to take into account only the dynamics of the reduced system spanned by the set of states  $|0,g\rangle$ ,  $|0,e\rangle$ ,  $|1,g\rangle$ , and  $|1,e\rangle$ . The graph associated to this case is shown in Fig. 1(b). The restricted dynamics neglects effects of second order in the coupling constant  $g$ . In particular, the evolution Eq. (1) written in this subspace preserves the trace of the density matrix equal to one up to terms that are second order in  $g$ . This simplified description contains several of the essential features of the global dynamics and makes it possible to obtain the stationary state of the system in an analytical form (see Sec. III).

In the case where a RWA cannot be assumed, the interaction Hamiltonian also connects the states  $|n,g\rangle$  and  $|n+1,e\rangle$  through nonresonant terms. The graph associated to this dynamics, restricted to the subspace with  $n=0$  and  $n=1$ , is shown in Fig. 1(c). The additional terms provide alternative mechanisms to achieve entanglement generation in the stationary state of the system and modify significantly the value of the entanglement obtained asymptotically.

As can be deduced from Fig. 1(a), if the HO were not coupled to a reservoir ( $v=0$ ) then the system would not reach a stationary state since the detector would tend to populate higher and higher energy levels and the mean phonon number will increase toward infinity. This case will be discussed in Sec. IV.

### III. RELATIVE ENTROPY OF ENTANGLEMENT

To characterize the amount of entanglement contained in the system, a particular protocol is defined and used in this work. First, for an arbitrary initial state, a projective measurement is performed onto the  $n$ -phonon manifold at a given time  $t$ . We will be mainly interested on values of  $t$  for which the stationary state of the system has been reached, although numerical results corresponding to projective measurements performed at a succession of different times has also been obtained and will be shown and discussed in Sec. IV. If the density matrix prior to this projection is denoted by  $\rho$ , then immediately after the measurement process the system is described by

$$\sigma_n = \frac{P_n \rho P_n}{\text{Tr}[P_n \rho P_n]} = A_n |n-1,e\rangle \langle n-1,e| + B_n |n-1,e\rangle \langle n,g| + B_n^* |n,g\rangle \langle n-1,e| + (1 - A_n) |n,g\rangle \langle n,g|, \quad (3)$$

with  $P_n \equiv |n-1,e\rangle \langle n-1,e| + |n,g\rangle \langle n,g|$  being the projector onto the  $n$ -phonon subspace. In fact, this projective measurement is not necessary in practice. The point that is addressed in this paper is that a given amount of entanglement will be available asymptotically in a particular subspace. Such entanglement could eventually be used by some quantum information protocol. However, one can think of this projection as an actual experimental step in some cases. If  $v \gg g, k$ , for instance, the population will be mainly concentrated in the subspace spanned by the four states  $\{|0,g\rangle, |0,e\rangle, |1,g\rangle, |1,e\rangle\}$ . Then,  $P_1$  can be realized by a

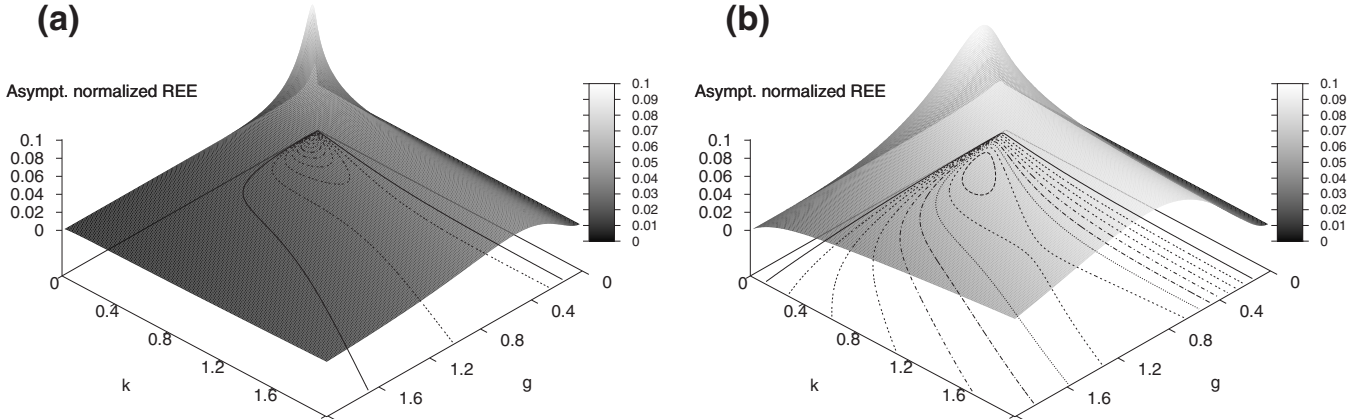


FIG. 2. Asymptotic value of the normalized relative entropy of entanglement, evaluated analytically by means of Eqs. (4)–(7), as a function of  $k$  and  $g$ , for (a)  $\nu=0.1$  and for (b)  $\nu=0.5$ . Dynamics restricted to the first four states and a rotating wave approximation are implicit in the analytical solution. In all panels, numerical values of  $k$ ,  $g$ , and  $\nu$  are given in units of  $\omega$ .

three-step procedure. (i) First, apply a so-called controlled-NOT gate that changes  $|0,g\rangle$  into  $|0,e\rangle$  and  $|0,e\rangle$  into  $|0,g\rangle$ , whereas it leaves  $|1,g\rangle$  and  $|1,e\rangle$  unchanged (see [4] for a proposal of an actual realization of a controlled-NOT gate in the context of quantum optics). (ii) Then, in a second step, the TLS is discarded if it is found in the excited state. (iii) Finally, a second controlled-NOT gate can be applied to the system. This protocol would project the state of the system onto the one-phonon subspace.

At this point, one may ask about the amount of entanglement that is available after the projective measurement. If the physical system is isolated from the different environments and under a RWA, an initially prepared state  $|0,e\rangle$  evolves in such a way that it will remain in the one-phonon manifold as a consequence of the fact that  $\frac{1}{2}\sigma_z + \alpha^\dagger\alpha$  is a constant of motion. In particular, at some time during its evolution, the system will be in the state  $\frac{1}{\sqrt{2}}(|0,e\rangle + |1,g\rangle)$ , which is maximally entangled. In this case, for the system in a pure state described by  $\sigma$ , entanglement is simply given by the von Neumann entropy of either of the two subsystems [32,33],  $E = -\text{Tr}[\sigma_a \ln \sigma_a] = -\text{Tr}[\sigma_o \ln \sigma_o]$ , with  $\sigma_a = \text{Tr}_o \sigma$  and  $\sigma_o = \text{Tr}_a \sigma$ . This quantity will oscillate with time between zero and its maximum value,  $E = \ln 2$ , with frequency  $g$ .

However there is not a unique definition of entanglement for a system in arbitrary mixed states as the ones generally obtained. In fact, most of the different definitions are quite difficult to evaluate even numerically in practice [5]. We will focus our interest in the quantity called REE evaluated in the one-phonon subspace, for which an analytical expression was obtained in Ref. [23]. For other definitions of entanglement, concurrence or entanglement of formation, for instance, the main results and qualitative conclusions of our study would also be applicable. The relative entropy of entanglement is defined as the minimum of a *distance* between the density matrix of the system,  $\sigma_n$ , and the set of all disentangled density matrices, where the distance (although not a metric) between two density operators,  $\sigma_n$  and  $\tilde{\sigma}_n$ , is given by the quantum relative entropy,  $d(\sigma_n \parallel \tilde{\sigma}_n) = \text{Tr}\{\sigma_n (\ln \sigma_n - \ln \tilde{\sigma}_n)\}$  [23].

For the stationary state mentioned in Sec. II, and after its projection onto the one-phonon subspace, the density matrix that describes the state of the system will have the form

$$\begin{aligned} \sigma_1^{ss} = & A_1|0,e\rangle\langle 0,e| + B_1|0,e\rangle\langle 1,g| + B_1^*|1,g\rangle\langle 0,e| + (1-A_1) \\ & \times |1,g\rangle\langle 1,g|, \end{aligned} \quad (4)$$

where the coefficients  $A_1$  and  $B_1$  are given by the expressions

$$\begin{aligned} A_1 = & \frac{1+g^2f(k,\nu)}{1+2g^2f(k,\nu)}, \\ B_1 = & \frac{g\nu[i(2k+\nu)+2][\nu(4k+\nu)+2i(2k+\nu)]}{\nu^3(4k+\nu)^2+4\nu(2k+\nu)^2+2g^2(k+\nu)(4k\nu+\nu^2+4)}, \end{aligned} \quad (5)$$

with

$$f(k,\nu) \equiv \frac{g^2(k+\nu)(4k\nu+\nu^2+4)}{\nu^3(4k+\nu)^2+4\nu(2k+\nu)^2}. \quad (6)$$

The better condition  $g \ll \omega, k, \nu$  is satisfied, the more accurate are the results obtained from these analytical expressions.

According to [23], for a reduced density matrix of this form the relative entropy of entanglement is given by the expression

$$E = e_+ \ln e_+ + e_- \ln e_- - A_1 \ln A_1 - (1-A_1) \ln (1-A_1), \quad (7)$$

where  $e_{\pm} = [1 \pm \sqrt{1-4[A_1(1-A_1)-|B_1|^2]}]/2$  are the eigenvalues of  $\sigma_1^{ss}$ .

Figures 2 and 3 show asymptotic values of the relative entropy of entanglement in the one-phonon subspace, multiplied by the corresponding population in that subspace, as a function of different parameters of the system. This quantity, which will be called “normalized” REE from now on, has been evaluated by means of formula (7) for the state given by Eqs. (4)–(6). All throughout the paper numerical values of  $g$ ,  $\nu$ , and  $k$  are given in units of  $\omega$ .

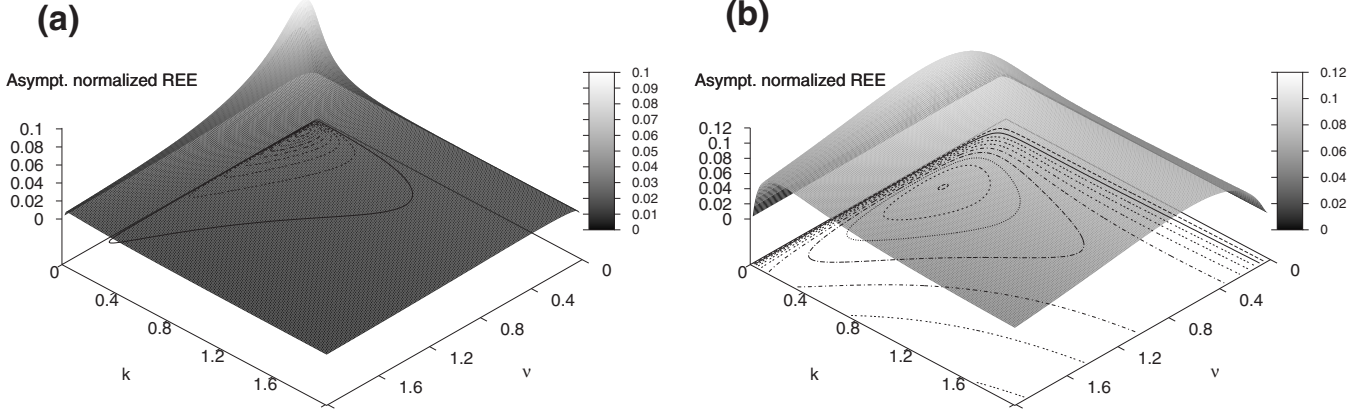


FIG. 3. Asymptotic value of the normalized relative entropy of entanglement, evaluated analytically by means of Eqs. (4)–(7), as a function of  $k$  and  $\nu$ , for (a)  $g=0.1$  and for (b)  $g=0.5$ . Dynamics restricted to the first four states and a rotating wave approximation are implicit in the analytical solution. ( $k$ ,  $g$ , and  $\nu$  are given in units of  $\omega$ .)

Although the analytical results shown in the figures are only quantitatively accurate for the weak-coupling regime discussed,  $g \ll \omega, k, \nu$ , the ranges in the plots have been chosen to ease a comparison with results presented in Sec. IV. Some qualitative features of the dynamics are correctly described by the evolution spanned by the states  $\{|0,g\rangle, |0,e\rangle, |1,g\rangle, |1,e\rangle\}$ . In particular, a localized maximum of the normalized REE is apparent close to the origin and a wider maximum is observed as  $k$  increases for intermediate values of  $g$ . Some other features will be made apparent and described in Sec. IV, superimposed on the ones observed here, when counter-rotating terms are taken into account. For a detailed analysis of the results and for a wider range of the model parameters, more states are involved in general and a numerical analysis has to be performed.

#### IV. NUMERICAL ANALYSIS

Numerical solutions for the state of the system as a function of time has been obtained by writing the master Eq. (1) in the truncated basis  $\{|n,g\rangle, |n,e\rangle; n=0, \dots, N\}$ , where  $N$  is chosen so that the results are independent of the exact value of  $N$ . Figure 4 shows the normalized relative entropy of entanglement in the one-phonon manifold as a function of time for a typical set of parameters characterizing the system and the initial state. In particular, the chosen value of  $g=0.1$  is such that a rotating wave approximation is applicable to simplify the interaction term  $H_I$ , although the actual calculations has been done without making such approximation. The system evolves toward a stationary state which contains a significant amount of REE only if both detector and bath are affecting the system. In other words, under RWA conditions, both environments are needed to generate entanglement in the system asymptotically.

The curves corresponding to cases where either no bath is present ( $\nu=0$ ) or no detector is present ( $k=0$ ) are shown for reference. The asymptotic state when  $k=0$  is  $|0,g\rangle$  only if the RWA is strictly valid. The small amount of REE remaining in this case as  $t \rightarrow \infty$  is a residual effect of the nonresonant terms present in  $H_I$ .

In the limiting case where  $\nu=0$  states with higher and higher phonon number become populated so that the relative entropy of entanglement in the particular subspace of interest goes to zero. There are numerical evidences that after an initial transient the variance of the state in Fock space,  $(\Delta N)^2$ , grows linearly with time, corresponding to normal diffusion. Since the spectrum of the number operator is bounded from below, the mean phonon number also increases in time.

The stationary state of the system can be efficiently obtained for different values of the relevant parameters by solving a set of coupled linear equations for  $\dot{\rho}=0$  in the truncated basis mentioned before. From this result asymptotic values of the REE can be directly obtained.

Figures 5(a) and 5(b) show asymptotic (stationary) results for the normalized relative entropy of entanglement in the one-phonon manifold vs  $g$  and  $k$  for two different values of  $\nu$ . The main features observed in these figures correspond to a double-peak structure, close to  $k=0$ , and a plateau appear-

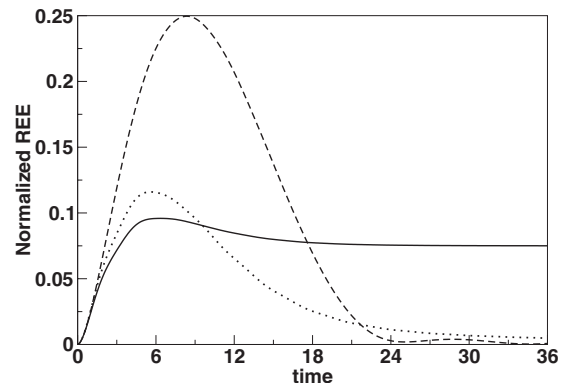


FIG. 4. Normalized relative entropy of entanglement in the one-phonon manifold versus time (solid line).  $g=\nu=k=0.1$ . The results corresponding to  $k=0$  and  $g=\nu=0.1$  (dashed line) and to  $\nu=0$  and  $g=k=0.1$  (dotted line) are plotted for reference. The initial state is  $\rho_0=(|0,g\rangle\langle 0,g|+|0,e\rangle\langle 0,e|)/2$ . Results were obtained by means of a “numerically” exact integration of Eq. (1) and no rotating wave approximation was used. ( $k$ ,  $g$ , and  $\nu$  are given in units of  $\omega$ , whereas time is expressed in units of  $\omega^{-1}$ .)

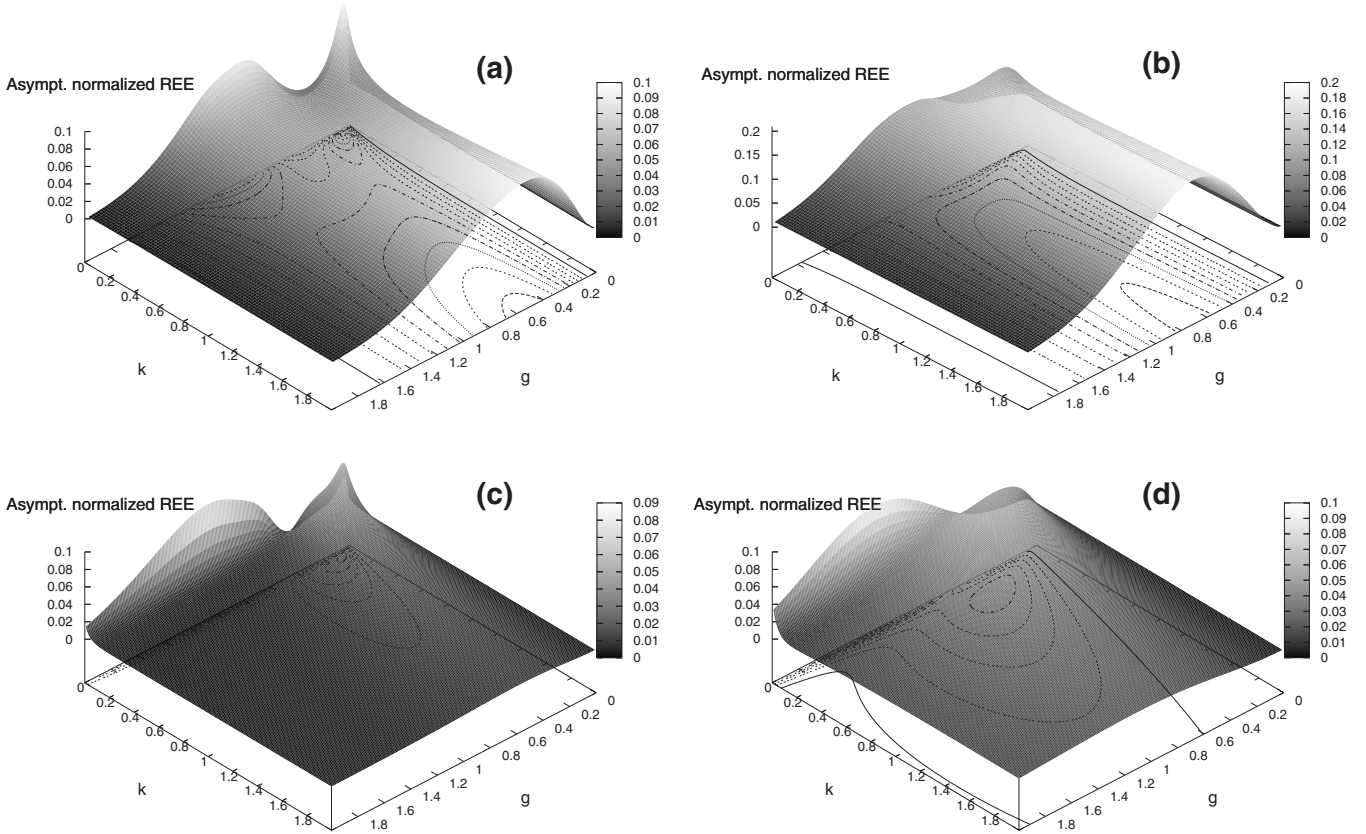


FIG. 5. Normalized asymptotic relative entropy of entanglement in the one-phonon manifold versus  $k$  and  $g$ . Panels (a) and (b) correspond to the case of a zero-temperature thermal bath with (a)  $\nu=0.1$  and (b)  $\nu=0.5$ . Panels (c) and (d) present results corresponding to the case of a thermal bath with mean phonon number  $\langle n \rangle=0.1$ . The results were obtained by means of a numerically exact integration of Eq. (1) for the cases in panels (a) and (b), and of Eq. (8) for those in panels (c) and (d). No rotating wave approximation was used. ( $k$ ,  $g$ , and  $\nu$  are given in units of  $\omega$ .)

ing as the parameter  $k$  is increased for intermediate values of  $g$ . As  $\nu$  increases the double-peak structure gets smoother and eventually disappears. The maximum values of the normalized REE are at least a factor of 2 larger for  $\nu=0.5$  than for  $\nu=0.1$ . Along the line  $k=0$ , the REE equals zero for  $g=0$ , since the stationary state is then given by  $|0,g\rangle$ . [In fact, the REE is zero for  $g=0$  independently of the value of  $k$  since then the two subsystems are not coupled and the steady state is given by  $\rho=(|0,g\rangle\langle 0,g|+|0,e\rangle\langle 0,e|)$ .] The entanglement increases with  $g$  until it reaches a maximum around  $g\simeq\nu$ . For larger values of  $g$  the nonresonant terms in the direct coupling between the HO and the TLS are responsible for a stationary state having nonzero REE. This is observed in the maximum appearing close to the  $k=0$  axis, centered around  $g\simeq\omega$  (which equals 1 in the present case). Let us mention that although the amount of entanglement is not zero for small values of  $g$ , and a double-peak structure is observed also along the line  $k=0$  due to the nonresonant terms in  $H_f$ , only the wide maximum survives as the REE is multiplied by the population of the corresponding subspace, which is greatly suppressed under the RWA valid for  $g\ll 1$ .

As the parameter  $k$  increases both peaks widen and a single plateau is observed corresponding to a case where both mechanisms,  $k$  measurements and nonresonant interaction terms, cooperate to generate a stationary state with a significant amount of entanglement over a large interval in  $g$

(see also Fig. 6, where a comparative of the effects corresponding to the different mechanisms involved is shown). Note however that this plateau was already observed under the RWA (see Fig. 2).

Figure 7 shows the asymptotic results for the normalized relative entropy of entanglement in the one-phonon manifold vs  $\nu$  and  $k$  for values of  $g=0.1$  and  $g=0.5$ .

As previously mentioned, values as high as 0.2 for the normalized REE (about 30% of its maximum possible value) are obtained when  $\nu\simeq 0.5$  [see Figs. 5(b) and 7(b)]. The increment in the value of the REE observed as  $\nu$  goes from 0.1 to 0.5 is due to an increment in the population of the  $n=0$  and  $n=1$  subspaces as the state gets localized in phonon space for a larger value of  $\nu$ . For an actual experiment that is intended to provide a source of entanglement, the parameter region corresponding to  $k\geq 1$  and  $g\simeq 0.5$ , observed in Fig. 5(a) for instance, should be preferred since the stationary state is obtained more rapidly as this rate is proportional to  $k^{-1}$ .

#### A. $\nu$ -reservoir finite-temperature effect

In general the  $\nu$  reservoir would be at a finite temperature. In order to study how this affects our results we consider a thermal bath with  $T\neq 0$ . Then the master equation that describes the evolution of the system has the form

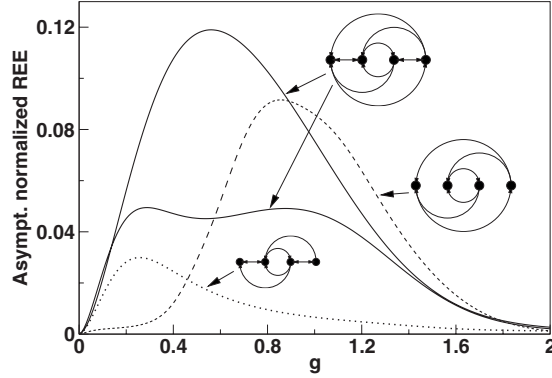


FIG. 6. Asymptotic values of the normalized relative entropy of entanglement in the one-phonon subspace vs  $g$ . The case where no measurement is performed on the system and nonresonant terms are kept is described by the dashed line. The dotted line presents results evaluated under the RWA when  $k=0.5$  for reference (accurate only for values of  $g \ll 1$ ). Finally, the solid lines represent cases where both mechanisms, nonresonant terms and  $k$  measurement, are affecting the dynamics of the system for different values of  $k=0.5$  (lower curve) and  $k=3.0$  (upper curve). Graphs describing the terms that are involved in each calculation are drawn for reference, although the actual calculations have been done with enough states to guarantee the convergence of the results. For all the calculations  $\nu$  has been set to 0.1. ( $k$ ,  $g$ , and  $\nu$  are given in units of  $\omega$ .)

$$\dot{\rho} = -i[H, \rho]/\hbar - k[\sigma_x, [\sigma_x, \rho]] + \nu(\langle n \rangle + 1)\mathcal{D}[a]\rho + \nu\langle n \rangle\mathcal{D}[a^\dagger]\rho, \quad (8)$$

where  $\langle n \rangle = e^{-\hbar\omega/k_B T}(1 - e^{-\hbar\omega/k_B T})^{-1}$  is the mean phonon number in the bath at frequency  $\omega$  and  $k_B$  is the Boltzmann constant. Figures 5(c) and 5(d) show how the temperature of the thermal bath affect the value of the asymptotic relative entropy of entanglement for one of the cases discussed before. In general, as temperature is increased, the peaked maximum that is observed close to the  $k=0$  axis widens as the thermal bath is less effective to drive the population to the one-phonon manifold. The peak is also shifted to a region with larger measurement strength  $k$ . The values obtained for the

asymptotic REE are also lowered in general as the population spreads over a larger parameter region.

On the other hand, the plateau appearing for larger values of  $k$  and intermediate coupling strength  $g$  is strongly suppressed as  $T$  increases. Nonetheless we may conclude that even at finite temperature there is a favorable set of parameters for which a significant amount of entanglement is available, specially in the region around the peaks observed in Figs. 5(c) and 5(d).

## V. CONCLUSIONS AND DISCUSSIONS

Manipulating entanglement is one of the main goals of many research works dealing with quantum processing of information. Characterizing and understanding the main features of this quantity and how it evolves are a key element of the field.

We have considered one of the simplest nontrivial model systems where entanglement generation and control are of interest. We have studied how different interactions between two subsystems and with a pair of reservoirs (related to relaxation of energy and to acquisition of information) provide mechanisms that allow some degree of control over the relative entropy of entanglement contained in the system as a function of time.

In particular, we have described quantitatively the relevance of the two environments to get, under certain approximations, a significant amount of entanglement asymptotically. We have found that although the nonresonant interaction terms are enough to generate entanglement on its own, the measurement process studied here allows for generating entanglement when its effect is combined with the effect of a reservoir even when a RWA is made for the interaction Hamiltonian. Moreover, both mechanisms,  $k$  measurement and nonresonant interaction terms, are found to cooperate to generate entanglement.

A remark on the role played by the measurement procedure is in order here. If the results obtained by the detector were not discarded then a different equation describes the dynamics of the system; the numerical results obtained then show that the REE fluctuates around the mean values ana-

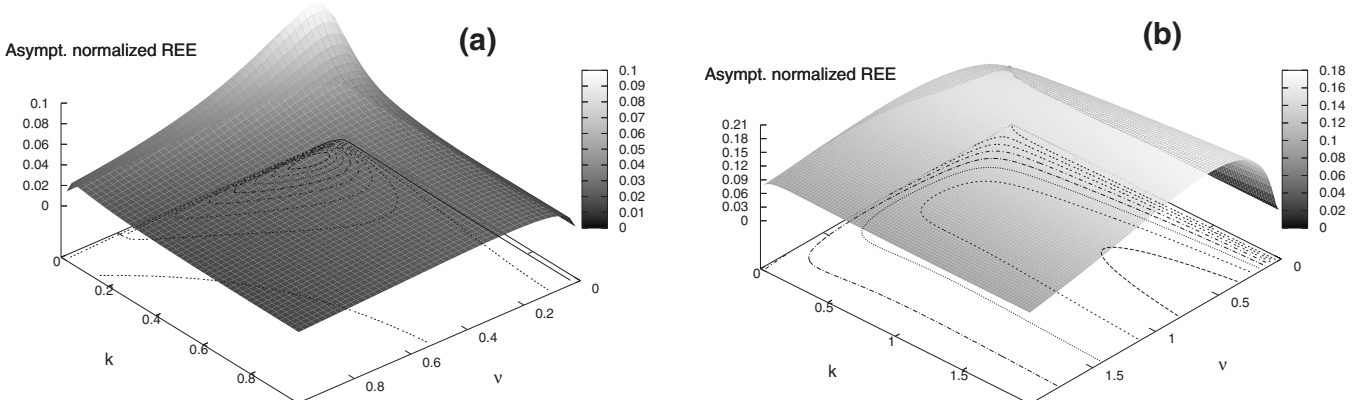


FIG. 7. Normalized asymptotic values of the relative entropy of entanglement in the one-phonon manifold versus  $\nu$  and  $k$ . Panel (a) corresponds to the case where  $g=0.1$ , whereas  $g=0.5$  for panel (b). These results are based on a numerically exact integration of Eq. (1), and no rotating wave approximation has been used. ( $k$ ,  $g$ , and  $\nu$  are given in units of  $\omega$ .)

lyzed here with a variance that is typically much smaller than the REE mean value, showing that the noisy evolution can be used to generate sensible values of entanglement. Furthermore, it would be interesting to study non-Markovian effects on the REE and search for a particular structured environment that may enhance the values of the REE.

## ACKNOWLEDGMENTS

Financial support was provided by Ministerio de Educación y Ciencia (Grants No. FIS2004-05687 and No. FIS2007-64018). One of us (E.H.-C.) thanks financial support from Ministerio de Educación y Ciencia under Grant No. BES 2005-7513.

- 
- [1] H.-K. Lo, S. Popescu, and T. Spiller, *Introduction to Quantum Computation and Information* (World Scientific, Singapore, 1998).
- [2] M. A. Nielsen and I. L. Chuang, *Introduction to Quantum Computation and Information* (Cambridge University Press, Cambridge, 2000).
- [3] G. Alber, T. Beth, M. Horodecki, P. Horodecki, R. Horodecki, M. Rötteler, H. Weinfurter, R. Werner, and A. Zeilinger, *Quantum Information: An Introduction to Basic Theoretical Concepts and Experiments* (Springer, New York, 2001).
- [4] J. I. Cirac and P. Zoller, Phys. Rev. Lett. **74**, 4091 (1995).
- [5] C. H. Bennett, D. P. DiVincenzo, J. A. Smolin, and W. K. Wootters, Phys. Rev. A **54**, 3824 (1996).
- [6] J. W. Pan, S. Gasparoni, R. Ursin, G. Weihs, and A. Zeilinger, Nature **423**, 417 (2003); J. W. Pan, Ch. Simon, C. Brukner, and A. Zeilinger, Nature (London) **410**, 1067 (2001).
- [7] D. Jonathan, M. B. Plenio, and P. L. Knight, Phys. Rev. A **62**, 042307 (2000).
- [8] A. N. Korotkov, Phys. Rev. B **63**, 115403 (2001).
- [9] D. F. Walls and G. J. Milburn, *Quantum Optics* (Springer, New York, 1994).
- [10] P. R. Rice, J. Gea-Banacloche, M. L. Terraciano, D. L. Freimund, and L. A. Orozco, Opt. Express **14**, 4514 (2006).
- [11] D. Leibfried, R. Blatt, C. Monroe, and D. Wineland, Rev. Mod. Phys. **75**, 281 (2003).
- [12] A. Wallraff, D. I. Shuster, A. Blais, L. Frunzio, R.-S. Huang, J. Majer, S. Kumar, S. M. Girvin, and R. J. Schoelkopf, Nature (London) **431**, 162 (2004).
- [13] A. Blais, R. S. Huang, A. Wallraff, S. M. Girvin, and R. J. Schoelkopf, Phys. Rev. A **69**, 062320 (2004).
- [14] M. Hofheinz, E. M. Weig, M. Ansmann, R. C. Bialczak, E. Lucero, M. Neeley, A. D. O'Connell, H. Wang, J. M. Martinis, and A. N. Cleland, Nature (London) **454**, 310 (2008).
- [15] A. D. Armour, M. P. Blencowe, and K. C. Schwab, Phys. Rev. Lett. **88**, 148301 (2002).
- [16] K. Jacobs, P. Lougovski, and M. Blencowe, Phys. Rev. Lett. **98**, 147201 (2007).
- [17] W. K. Hensinger, D. W. Utami, H. S. Goan, K. Schwab, C. Monroe, and G. J. Milburn, Phys. Rev. A **72**, 041405(R) (2005).
- [18] L. Tian and P. Zoller, Phys. Rev. Lett. **93**, 266403 (2004).
- [19] I. Wilson-Rae, P. Zoller, and A. Imamoglu, Phys. Rev. Lett. **92**, 075507 (2004).
- [20] M. B. Plenio and S. F. Huelga, Phys. Rev. Lett. **88**, 197901 (2002).
- [21] H. Nha and H. J. Carmichael, Phys. Rev. Lett. **93**, 120408 (2004).
- [22] I. Sinaysky, F. Petruccione, and D. Burgarth, Phys. Rev. A **78**, 062301 (2008).
- [23] V. Vedral and M. B. Plenio, Phys. Rev. A **57**, 1619 (1998).
- [24] W. H. Louisell, *Quantum Statistical Properties of Radiation* (Wiley, New York, 1973).
- [25] H. Carmichael, *An Open Approach to Quantum Optics* (Springer-Verlag, Berlin, 1991).
- [26] K. Jacobs, A. N. Jordan, and E. K. Irish, Europhys. Lett. **82**, 18003 (2008).
- [27] M. Sarovar, H.-S. Goan, T. P. Spiller, and G. J. Milburn, Phys. Rev. A **72**, 062327 (2005).
- [28] A. C. Doherty and K. Jacobs, Phys. Rev. A **60**, 2700 (1999).
- [29] H. M. Wiseman and G. J. Milburn, Phys. Rev. A **47**, 642 (1993).
- [30] K. Jacobs and D. A. Steck, Contemp. Phys. **47**, 279 (2006).
- [31] N. Gisin and Ian C. Percival, J. Phys. A: Math. Gen. **25**, 5677 (1992); **26**, 2233 (1993); **26**, 2245 (1993).
- [32] C. H. Bennett, H. J. Bernstein, S. Popescu, and B. Schumacher, Phys. Rev. A **53**, 2046 (1996).
- [33] S. Popescu and D. Rohrlich, Phys. Rev. A **56**, R3319 (1997).